Journal of Soil Sciences and Agricultural Engineering

Hydrogen Production Enhancement in Pine Sawdust Gasification by Numerical and Experimental Methods

Jado A. [1]*; Tatiana Morosuk[2] and Jinming Pan[3]

[1] Mansoura University, Department of Agricultural Engineering, Mansoura 35516, Egypt
[2] Institute for Energy Engineering, Technical University of Berlin, Berlin 10587, Germany
[3] Zhejiang University, Department of Biosystems Engineering, Hangzhou 310058, China

Cross Mark

ABSTRACT

This research comprehensively investigates hydrogen production optimization in pine sawdust gasification through integrated numerical simulation and experimental validation. The numerical model, developed using Aspen Plus®, demonstrated exceptional correlation with experimental data ($R^2 > 0.95$) at 800°C, validating its predictive capability. Parametric analysis revealed that elevating the reaction temperature from 600°C to 800°C significantly enhanced H_2 concentration from 31.12 vol% to 35.11 vol%, primarily due to the acceleration of endothermic water-gas shift (WGS) and steam reforming reactions. The equivalence ratio (ER) exhibited an inverse relationship with H_2 yield, where increasing ER from 0.2 to 0.4 resulted in a substantial decrease in H_2 concentration from 37.61 vol% to 30.07 vol%, attributed to the diminished steam availability for reforming reactions. Furthermore, augmentation of the steam-to-biomass (S/B) ratio from 0.5 to 1.7 facilitated increased H_2 concentration from 35.28 vol% to 37.22 vol%, owing to enhanced steam reforming and WGS reaction kinetics. Through multi-parameter optimization, optimal conditions were established at temperature: 750-800°C, ER: 0.2-0.25, and S/B ratio: 1.1-1.4, achieving maximum H_2 concentrations of 36-38 vol%.

Keywords: Hydrogen production; Gasification; Pine sawdust; Numerical modeling

INTRODUCTION

Biomass, a renewable energy source derived from organic materials, continues to be one of the most significant contributors to global energy production, ranking third after coal and oil (Elsaddik et al., 2024; Dash et al., 2023). During photosynthesis, biomass captures atmospheric CO_2, which is released back into the environment upon combustion. This cyclical process renders biomass a carbon-neutral energy source, positioning it as a promising alternative to fossil fuels in the context of escalating concerns over climate change (Bachs-Herrera et al., 2023; Salas et al., 2024). Recent studies emphasize the potential of agricultural residues, such as straw, bagasse, and husks, as well as by-products from forestry and wood-processing industries, including wood chips, sawdust, and bark, as viable biomass energy sources (Liu & Yu, 2021; Monteiro et al., 2023). These materials offer a sustainable energy solution, improving waste management and resource efficiency (De Faria et al., 2021).

Biomass gasification has emerged as a prominent thermochemical conversion technology for sustainable energy production due to its ability to reduce pollutant emissions, such as nitrogen oxides (NO_x) and sulfur oxides (SO_x), while achieving higher gas production efficiency compared to pyrolysis and combustion (Winchell et al., 2022; Wang et al., 2020). This process minimizes environmental impacts and enhances overall plant efficiency by utilizing the produced gas in turbines and engines for electricity generation (Indrawan et al., 2020; Faheem et al., 2024). The primary outputs of biomass gasification include a gas mixture of hydrogen, methane, carbon dioxide, and carbon monoxide, along with by-products such as char and tar (Shahbeig et al., 2022; Siwal et al., 2020).

The quality of the gasification products is significantly influenced by operating parameters, such as the equivalence ratio (ER), steam-to-biomass ratio (S/B), bed material, temperature, particle size, and biomass carbon content (Gao et al., 2021; Zhang et al., 2020; Xiang et al., 2020). For instance, ER has been shown to negatively affect methane content and lower heating value (LHV), while S/B positively influences hydrogen concentration in the product gas (Chojnacki et al., 2020; Nguyen, 2024). Understanding and optimizing these parameters are crucial for improving the efficiency and sustainability of the gasification process.

Process simulation has become indispensable, offering independence from feedstock types and experimental locations and significant time and cost savings (Zhang et al., 2021). The use of Aspen Plus® software for the development of gasification models has been the subject of extensive research in recent years (González-Vázquez et al., 2021; Marcantonio et al., 2019; Nguyen et al., 2021). Aspen Plus®, a widely used simulation software, has proven effective in modeling and optimizing biomass gasification processes, enabling researchers to predict outcomes and refine operational parameters (Zaman & Ghosh, 2023). Several researchers have focused on model validation and techno-economic assessments, while others have investigated specific process enhancements, including CO_2 capture integration and gasification agent optimization (Mighani et

al., 2020). Begum et al. (2013) utilized the Gibbs free energy minimization method to simulate the gasification process in a fixed-bed gasifier with various feedstocks, including coffee bean husks, municipal solid waste (MSW), wood, and green wastes as well as investigated the influence of temperature and air-fuel ratio. Abdelouahed et al. (2012) developed a simulation model based on the kinetic method, using FORTRAN files to input information about reactor computation and chemical kinetics to investigate the biomass gasification process in a dual fluidized bed (DFB) gasifier.

More recently, Ainouss et al. (2020) compared the gasification results of coir pith with its char and conducted a techno-economic and sensitivity analysis using Aspen Plus®, revealing that the gasification of biomass char was more advantageous than biomass alone. Xiang et al. (2020) studied the influence of different gasification agents (steam, CO_2, steam-O_2, CO_2-O_2, steam-CO_2, and steam-CO_2-O_2) using Aspen Plus®, finding that steam could promote the generation of H2 but inhibit the production of CO, while CO_2 contributed to the yield of CO, and the introduction of O_2 could significantly reduce the yield of CO and CH_4.

The challenge in biomass gasification processes is understanding how various operating parameters, such as temperature, equivalence ratio, and steam-to-biomass ratio, affect the product gas composition. Efficient optimization of these parameters is crucial for maximizing the energy output and effectiveness of biomass gasification. Current methods may lack detailed insights into the impacts of these parameters, thereby limiting the efficiency and yield of desirable gases like hydrogen. Many researchers have ignored the formation of tar, leading to differences between predicted results and reality.

Therefore, the present study aims to model and analyze biomass gasification processes using the Aspen Plus® simulator. The study investigates the effects of operating parameters on product gas composition within a fluidized bed reactor. By conducting simulations and experimental studies, particularly using Pine Sawdust as a raw material, the research seeks to provide insights on optimizing biomass gasification to improve energy production efficiency and gas yield, mainly hydrogen.

MATERIALS AND METHOD

Experimental Setup and Methodology

The experimental study employed a pilot-scale atmospheric fluidized bed gasification system designed for continuous operation, featuring a reactor assembly with a biomass feeding mechanism (variable-speed screw feeder), bed material feeding system, air distribution via a bubble cap, and steam injection (Figure 1). The system operated within a temperature range of 600−800 °C and equivalence ratios of

0.20−0.4, using Pine Sawdust as biomass and silica sand as the bed material. The process began with the introduction of silica sand, followed by initial heating with LPG at 15−20 L·h^{-1} until the desired temperature was reached, after which Pine Sawdust was fed into the reactor. Key parameters, biomass feed rate (controlled by screw speed), air flow rate, and steam flow rate (monitored via calibrated orifice meters), were continuously adjusted to optimize gasification. The product gas underwent multi-stage cleaning, including cyclone separation, water-based scrubbing, secondary filtration, and moisture removal with silica gel, before being analyzed for H_2, CO, CH_4, and CO_2 using a calibrated infrared analyzer. Temperature profiles, pressure differentials, and flow rates were continuously monitored, and all measurements were recorded under steady-state conditions to ensure accuracy and reproducibility. This setup enabled a systematic investigation of the effects of operating parameters on gasification performance.
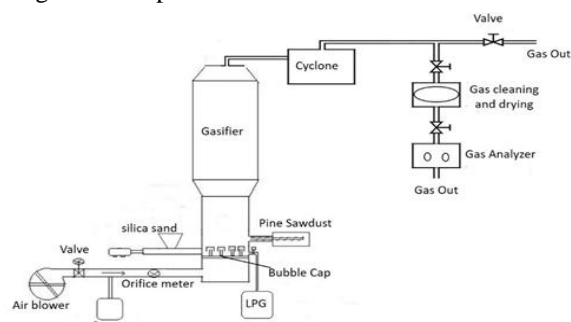

Fig. 1 System diagram of the experimental setup

Model Description and Simulation Framework

Aspen Plus® simulation software was employed to replicate the auto thermal pilot-scale bubbling fluidized bed. A sequential modular simulation strategy was devised to model a fluidized bed reactor by segmenting it into multiple blocks, thereby aiding model convergence. The simulation encompassed the process partitioned into three continuous sub-processes: the pyrolysis process B1 and B2, which also includes the drying phase, the oxidation process B3, and the reduction process B4, as outlined in the schematic of Figures 2 and detailed in Table 1 and Table 2. Additionally, Table 3 presents the Characteristics of pine sawdust. The kinetic parameters and associated chemical reaction mechanisms implemented in the gasification model were adapted from the comprehensive framework established by Puig-Gamero et al. (2021), wherein the reaction kinetics and thermodynamic equilibrium conditions were systematically evaluated under controlled operational parameters.
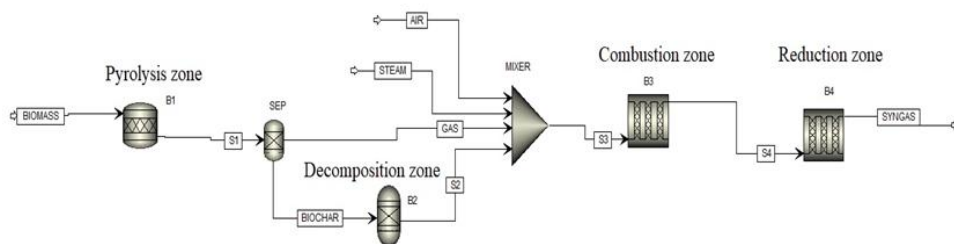

Fig. 2 The process flowsheet of the simulation model for the gasification operation

Table 1. Various Unit Blocks Utilized in the Model

Name	Type	Scheme	Description
B1	RSTOIC	B1	The char was broken down into its individual components, including ash, and the process was conducted at atmospheric pressure with temperatures ranging from 600 to 800 °C, depending on the simulation.
SEP	SEP	SEP	Separator of char and gas product
B2	RYIELD	B2	The biomass pyrolysis reactor utilized an Excel subroutine to break down biomass into pyrolytic compounds, operating at atmospheric pressure with temperatures ranging from 600 to 800 °C, depending on the simulation.
B3	RPLUG	B3	The gasifier reactor modeled the oxidation zone, incorporating the actual temperature profile, reactor dimensions, and kinetic parameters for each reaction. It operated at atmospheric pressure with temperatures ranging from 600 to 800 °C, depending on the simulation.
B4	RPLUG	B4	The gasifier reactor represented the reduction zone, with the actual temperature profile, reactor dimensions, and kinetic parameters for each reaction explicitly defined. It operated at atmospheric pressure with temperatures ranging from 600 to 800 °C, depending on the simulation.

Table 2 Environmental conditions and operational parameters defined for the simulation

Operating Parameters	Value
Environmental temperature	25 °C
Environmental pressure	1 atm
Gasification temperature	600,650,700,750,800
Air equivalent ratio	0.2, 0.25, 0.30, 0.35, 0.40
Steam biomass ratio	0.50, 0.80, 1.10, 1.40, 1.70

Table 3. Proximate and elemental analysis of the pine sawdust

Proximate analysis (wt % dry basis)	
Volatile matter	80.25
Fixed carbon	19.10
Ash	0.65
Ultimate analysis (wt % dry basis)	
C	50.11
H	8.13
O	41.12
N	0.14
S	0.50

In the simulation, biomass and char were treated as non-conventional components, with their proximate and elemental analyses defined using the ULTANAL and PROXANAL models. The HCOALGEN and DCOALIGT models were used to determine the enthalpy and density of these non-conventional components, respectively. HCOALGEN includes various correlations to calculate heat capacity, heat of combustion, and heat of formation. The heat of formation is derived from the biomass's heat of combustion and the formation enthalpy of the products of the gasification process. The heat of combustion is calculated using the proximate and elemental composition of the biomass, utilizing multiple correlations available in Aspen Plus® (Abdelouahed et al., 2012). The DCOALIGT model, based on the Institute of Gas Technology (IGT) correlation, requires ULTANAL data. Ash was also treated as a non-conventional component, with its ultimate and proximate analyses set to 100%. The Peng-Robinson fluid-dynamic package with the Boston-Mathias function was selected as it is deemed most suitable for high-temperature gasification processes (Pala et al., 2017). Compounds such as H_2, O_2, CO, CO_2, CH_4, C_2H_4, H_2O, N_2, NH_3, C_6H_6, C_6H_6O, and $C_{10}H_8$ were defined as fluids, while elemental C and S were designated as solids.

Model assumptions

The development of a fixed-bed gasification model in Aspen Plus® follows a systematic approach begins with selecting and integrating appropriate functional modules that represent the physical process interconnected through material streams. The model's thermodynamic framework is established by specifying suitable property methods. However, a complete replication of actual reaction pathways is not feasible due to the intricate nature of the reaction mechanisms in real-world gasification and the inherent constraints of simulation software capabilities. Consequently, the process necessitates strategic simplification based on well-defined assumptions. Table 4 presents the fundamental assumptions implemented in this study for modeling the fixed-bed pyrolysis gasification process within the Aspen Plus®.

Table 4. Assumptions Used in the Model

Model Assumptions

- Ash exhibited inert behavior
- The process operated under steady-state conditions
- The reactor maintained uniform internal pressure distribution
- The reactor system was considered adiabatic and isobaric
- All gaseous components demonstrated ideal gas behavior
- The formation of NH3 and H2S was neglected in the model
- The product stream contained residual unconverted solid carbon
- The tar composition was simplified to comprise C6H6, C6H6O, and C10H8
- A one-dimensional (1D) modeling approach was implemented
- The model excluded fluidization velocity within the reactor as a parameter
- All chemical reactions were governed by Arrhenius kinetics

Methodology for Model Development

Table 1 provides a concise description of the blocks utilized in the model. Biomass (Stream 1) was introduced at ambient conditions (25 °C and 1 atm) into block B1 to simulate instantaneous drying and pyrolysis. The Aspen Plus® modeling framework treats the drying and devolatilization processes as two independent, time-independent steps designed to supply water and pyrolysis products as inputs for the subsequent gasification model. The drying and pyrolysis processes were modeled using an

established approach (Neves et al., 2011), which provided data on char, gas, and tar products. This data was processed through an external Excel subroutine, supporting the Aspen Plus® model. The model predicts the yields and elemental composition of pyrolysis products, represented by eight species: tar (a mixture of C_6H_6, $C_{10}H_8$, and C_6H_6O), H_2, H_2O, CO, CO_2, CH_4, and dry ash-free char. The mass balance was adjusted to calculate the percentage of each compound. A system of linear equations was formulated into an empirical model, following the methodological approach outlined by Neves et al. (2011).

Block B2 was designed to decompose char into its constituent compounds. Subsequently, the char oxidation process was modeled in block B3 to achieve the gasification temperature, enabling an autothermal gasification process. The primary gas produced in the oxidation zone and the residual char were then fed into block B4, representing the reduction reactions occurring within the gasifier. Air and steam, introduced at 1 bar and 25 °C (stream 5), were supplied to the reactor represented by block B3. Both B3 and B4 blocks were simulated using the R-Plug module, which models an ideal reactor operating under specified conditions. The accurate temperature profile and reactor dimensions (reaction chamber with an internal diameter of 0.25 m and a height of 2.3 m) were explicitly defined, along with the kinetic parameters for each reaction. The reactions and their associated kinetic parameters used in the gasification process were sourced from Puig-Gamero et al. (2021).

RESULTS AND DISCUSSIONS

Model validation

As shown in Figure 3, the simulation results strongly agree with the experimental data at 800°C, confirming the model's reliability. However, some discrepancies are observed, particularly in the concentrations of CO and CO_2. The simulated CO concentration is higher, while CO_2 is lower than experimental values.
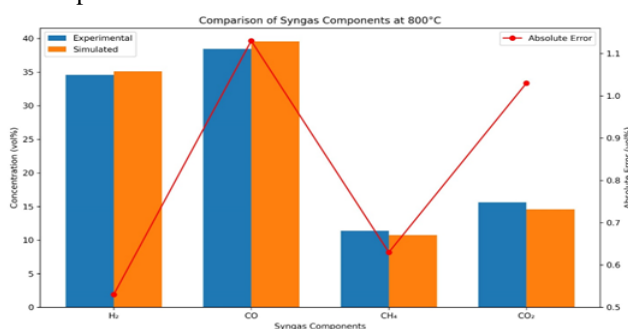
Fig. 3. Comparison of Syngas Component Concentrations and Errors Between Experimental and Simulated Data

This difference arises because the simulation assumes incomplete combustion of carbon under oxygen-deficient conditions, as the gasifying agent input limits complete biomass burning. Consequently, the model predicts elevated CO and reduced CO_2 levels. Similarly, the simulated H_2 concentration slightly exceeds experimental values due to the model's exclusion of tar and other hydrocarbons (e.g., C_nH_m), which leads to a higher predicted H_2 content based on the element balance principle. In the experimental process, CH_4 is produced during both the pyrolysis reaction and the methane reforming stage. This additional CH_4 production during pyrolysis leads to higher methane content in the experimental results compared to the simulation. The absolute error analysis highlights the accuracy of the model, with errors remaining below 2% for all components.

This level of precision is acceptable for practical applications and suggests that the model can be used to optimize gasification parameters.

Effect of Operating Conditions on Syngas Production
Effect of Varying Temperature on Syngas Production

As shown in Figure 4, the line chart demonstrates the variation in gas composition (H2, CO, CH4, and CO2) with increasing temperature during the gasification process. Hydrogen concentration shows a consistent increase, rising from 31.12 vol% at 600°C to 35.11 vol% at 800°C. This trend is attributed to the enhanced water-gas shift reaction and steam reforming at higher temperatures, which favor hydrogen production. Conversely, CO concentration decreases steadily from 42.34 vol% to 39.56 vol%, indicating the consumption of CO in the water-gas shift reaction. CH_4 exhibits a gradual decline, reflecting the thermal cracking and reforming of hydrocarbons at elevated temperatures. CO_2 remains relatively stable, with a slight increase, suggesting its role as a by-product of the water-gas shift reaction and partial oxidation.

The observed trends highlight the critical role of temperature in optimizing gasification efficiency and product gas quality. The increase in hydrogen concentration with temperature is particularly significant for applications requiring high hydrogen content, such as fuel cells and synthetic fuel production. The reduction in methane and carbon monoxide concentrations at higher temperatures indicates improved conversion efficiency and reduced tar formation, which is desirable for cleaner and more efficient gasification. The relatively stable carbon dioxide levels suggest that the process achieves a balance between oxidation and reforming reactions. These findings underscore the importance of temperature control in achieving the desired syngas composition and maximizing the overall efficiency of the gasification process.
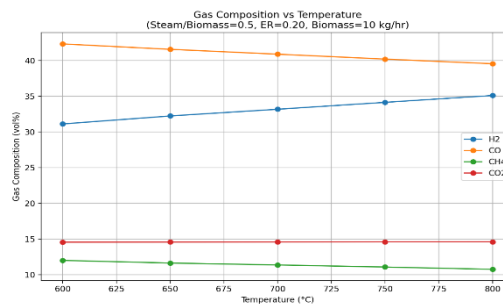
Fig. 4. Variation of Product Gas Composition with Temperature

Effect of Varying Equivalence Ratio on Syngas Production

As shown in Figure 5, the line plot depicts the changes in gas composition (H_2, CO, CH_4, and CO_2) as the equivalence ratio (ER) increases during the gasification process at 800°C. The hydrogen (H2) concentration decreases consistently from 37.61 vol% at an ER of 0.2 to 30.07 vol% at an ER of 0.4. This reduction is mainly due to the diminished availability of steam for the water-gas shift reaction and steam reforming with higher equivalence ratios. Similarly, carbon monoxide (CO) shows a slight reduction from 39.97 vol% to 38.91 vol%, indicating a change in the balance of reactions. Methane (CH_4), on the other hand, remains relatively constant at around 10.74 vol%, suggesting that the ER has a limited effect on hydrocarbon cracking under these conditions. Conversely, carbon dioxide (CO_2) concentration increases markedly, from 11.63 vol% to 20.31 vol%, indicating a boost in partial oxidation reactions at

higher equivalence ratios. These patterns underscore the pivotal role of the equivalence ratio in defining syngas composition and the overall efficiency of the gasification process. The drop in hydrogen concentration with higher ER signals a compromise between hydrogen production and the extent of oxidation reactions. The steady methane levels suggest that ER has little impact on hydrocarbon reforming, which could be beneficial for maintaining a consistent syngas quality. However, the significant rise in carbon dioxide concentration at higher ERs highlights the predominance of oxidation reactions, which may lower the calorific value of the syngas. These insights imply that operating at lower ERs (e.g., ER = 0.2) is preferable for producing hydrogen-rich syngas. In comparison, higher ERs might be advantageous for applications that require more CO_2, such as enhanced oil recovery or carbon capture and storage.
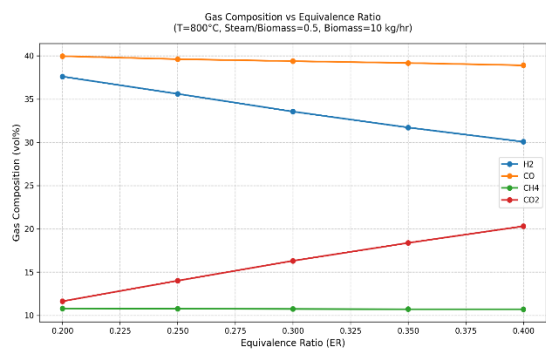

Fig. 5. Variation of Product Gas Composition with Equivalence Ratio

Effect of Varying Steam to Biomass Ratio on Syngas Production

As shown in Figure 6, the line chart illustrates the variation in gas composition (H_2, CO, CH_4, and CO_2) with increasing steam-to-biomass ratio (S/B) during the gasification process at 800°C. Hydrogen (H_2) concentration increases steadily from 35.28 vol% at S/B = 0.5 to 37.22 vol% at S/B = 1.7, reflecting enhanced steam reforming and water-gas shift reactions at higher S/B ratios. Carbon monoxide (CO) shows a slight decrease from 39.68 vol% to 39.01 vol%, indicating a shift in equilibrium favoring hydrogen production. Methane (CH_4) remains relatively stable at

around 10.71 vol%, suggesting the limited influence of S/B ratio on hydrocarbon cracking under the given conditions. Carbon dioxide (CO_2) concentration decreases from 14.29 vol% to 13.08 vol%, likely due to its consumption in the water-gas shift reaction.

These trends highlight the critical role of the steam-to-biomass ratio in optimizing the syngas composition and gasification efficiency. Higher S/B ratios favor hydrogen-rich syngas production, which is advantageous for fuel cells and synthetic fuel synthesis applications. The slight decrease in CO and CO_2 concentrations at higher S/B ratios suggests improved carbon conversion efficiency and reduced greenhouse gas emissions. The relatively stable methane levels indicate consistent syngas quality across the S/B range, making the process adaptable to various industrial applications. These findings underscore the importance of controlling the S/B ratio to achieve the desired syngas composition and maximize the overall efficiency of the gasification process.
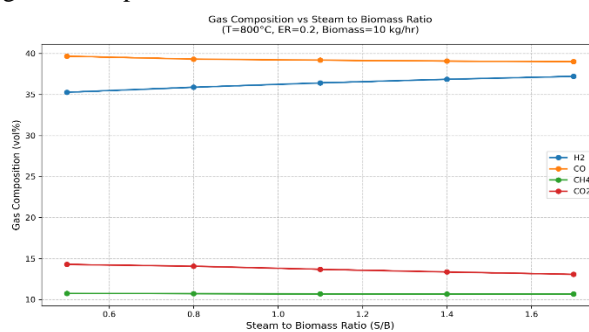

Fig. 6. Variation of Product Gas Composition with steam to biomass ratio

Effect of Operating Parameters on Hydrogen Production

The influence of operating parameters on hydrogen content during biomass gasification was investigated through a series of contour plots, as shown in Figure 7. The analysis covered temperature ranges from 600°C to 800°C, equivalence ratios (ER) from 0.2 to 0.4, and steam-to-biomass (S/B) ratios varying from 0.5 to 1.4.
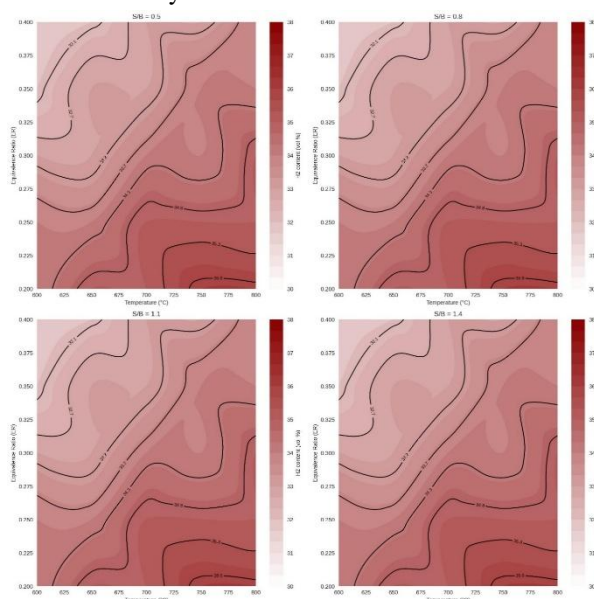

Fig. 7 Effect of gasification temperature on H₂ content in air-steam gasification

The contour plots demonstrate a consistent positive correlation between temperature and H_2 content for all S/B

ratios. As the temperature increased from 600°C to 800°C, H_2 content showed improved, with maximum values reaching

approximately 38 vol%. This trend is attributed to the endothermic nature of steam reforming and water-gas shift reactions, which are favored at higher temperatures.

A notable inverse relationship was observed between ER and H_2 content. The highest H_2 concentrations were achieved at lower ER values (around 0.2) while increasing ER to 0.4 led to decreased H_2 production. This phenomenon can be explained by the dominance of oxidation reactions at higher ER values, which consume part of the feedstock and reduce the potential for H2 formation.

The four subplots illustrate the system's response to varying S/B ratios (0.5, 0.8, 1.1, and 1.4). Higher S/B ratios generally resulted in improved H2 content, particularly evident in the transition from S/B = 0.5 to 1.4, where maximum H_2 concentrations increased by approximately 2-3 vol%. This enhancement can be attributed to the promotion of steam reforming and water-gas shift reactions, which are key pathways for H_2 production.

The optimal conditions for maximizing H_2 content were identified at temperature: 750-800°C, ER: 0.2-0.25, and S/B ratio: 1.1-1.4. Under these conditions, H_2 content reached its peak values of 36-38 vol%. The contour patterns suggest that further increases in temperature beyond 800°C might yield additional improvements in H2 content, though this would need to be balanced against energy efficiency considerations and material constraints.

CONCLUSION

This investigation elucidates the fundamental relationships between operational parameters and H_2 production efficiency in pine sawdust gasification systems. The study empirically demonstrates that thermal elevation and increased steam-to-biomass ratios synergistically increase H_2 yield by promoting of endothermic reactions, while elevated equivalence ratios adversely affect H_2 production due to competitive oxidation reactions. The validated numerical model demonstrates strong predictive capabilities, enabling precise parameter optimization for maximum H_2 yield. These findings provide crucial insights for scaling up and industrial implementation of biomass gasification systems, particularly for fuel cell technologies and synthetic fuel production applications. Additionally, the established mathematical correlations between operational parameters and H_2 yield contribute to the theoretical framework for future biomass gasification research. The optimized conditions identified in this study represent a significant advancement toward the development of more efficient and environmentally sustainable hydrogen production technologies through biomass utilization. Future research directions may focus on catalyst integration and optimizing reactor design to further enhance H_2 selectivity and process efficiency.

REFERENCES

Abdelouahed, L., Authier, O., Mauviel, G., Corriou, J. P., Verdier, G., & Dufour, A. (2012). Detailed modeling of biomass gasification in dual fluidized bed reactors under Aspen plus. *Energy & Fuels*, *26*(6), 3840-3855. https://doi.org/10.1021/ef300411k

Alnouss, A., Parthasarathy, P., Shahbaz, M., Al-Ansari, T., Mackey, H., & McKay, G. (2020). Techno-economic and sensitivity analysis of coconut coir pith-biomass gasification using ASPEN PLUS. *Applied Energy*, *261*, 114350. https://doi.org/10.1016/j.apenergy.2019.114350

Bachs-Herrera, A., York, D., Stephens-Jones, T., Mabbett, I., Yeo, J., & Martin-Martinez, F. J. (2023). Biomass carbon mining to develop nature-inspired materials for a circular economy. *iScience*, *26*(4), 106549. https://doi.org/10.1016/j.isci.2023.106549

Begum, S., Rasul, M., Akbar, D., & Ramzan, N. (2013). Performance analysis of an integrated fixed bed gasifier model for different biomass feedstocks. *Energies*, *6*(12), 6508-6524. https://doi.org/10.3390/en6126508

Chojnacki, J., Najser, J., Rokosz, K., Peer, V., Kielar, J., & Berner, B. (2020). Syngas composition: Gasification of wood pellet with water steam through a reactor with continuous biomass feed system. *Energies*, *13*(17), 4376. https://doi.org/10.3390/en13174376

Dash, S. K., Chakraborty, S., & Elangovan, D. (2023). A brief review of hydrogen production methods and their challenges. *Energies*, *16*(3), 1141. https://doi.org/10.3390/en16031141

De Faria Ferreira Carraro, C., Celestino Martins, A., Carolina da Silva Faria, A., & Cristina Almeida Loures, C. (2021). Agroenergy from residual biomass: Energy perspective. *Biotechnological Applications of Biomass*. https://doi.org/10.5772/intechopen.93644

Elsaddik, M., Nzihou, A., Delmas, G., & Delmas, M. (2024). Renewable and high-purity hydrogen from lignocellulosic biomass in a biorefinery approach. *Scientific Reports*, *14*(1). https://doi.org/10.1038/s41598-023-50611-5

Faheem, H. H., Britt, B., Rocha, M., Zhou, S., Li, C., Cai, W., & Fan, L. (2024). Sensitivity analysis and process optimization for biomass processing in an integrated gasifier-solid oxide fuel cell system. *Fuel*, *356*, 129529. https://doi.org/10.1016/j.fuel.2023.129529

Gao, N., Chen, C., Magdziarz, A., Zhang, L., & Quan, C. (2021). Modeling and simulation of pine sawdust gasification considering gas mixture reflux. *Journal of Analytical and Applied Pyrolysis*, *155*, 105094. https://doi.org/10.1016/j.jaap.2021.105094

González-Vázquez, M., Rubiera, F., Pevida, C., Pio, D. T., & Tarelho, L. A. (2021). Thermodynamic analysis of biomass gasification using Aspen plus: Comparison of stoichiometric and non-stoichiometric models. *Energies*, *14*(1), 189. https://doi.org/10.3390/en14010189

Indrawan, N., Kumar, A., Moliere, M., Sallam, K. A., & Huhnke, R. L. (2020). Distributed power generation via gasification of biomass and municipal solid waste: A review. *Journal of the Energy Institute*, *93*(6), 2293-2313. https://doi.org/10.1016/j.joei.2020.07.001

Liu, W., & Yu, H. (2021). Thermochemical conversion of Lignocellulosic biomass into mass-producible fuels: Emerging technology progress and environmental sustainability evaluation. *ACS Environmental Au*, *2*(2), 98-114. https://doi.org/10.1021/acsenvironau.1c00025

Marcantonio, V., Bocci, E., & Monarca, D. (2019). Development of a chemical quasi-equilibrium model of biomass waste gasification in a fluidized-bed reactor by using Aspen plus. *Energies*, *13*(1), 53. https://doi.org/10.3390/en13010053

Mighani, M., Covella, K., Örs, E., Rauch, J., Mönch, H., & Gräbner, M. (2020). undefined. *Computer Aided Chemical Engineering*, 1279-1284. https://doi.org/10.1016/b978-0-12-823377-1.50214-7

Monteiro, A. R., Battisti, A. P., Valencia, G. A., & De Andrade, C. J. (2023). The production of high-added-Value Bioproducts from non-conventional biomasses: An overview. *Biomass*, *3*(2), 123-137. https://doi.org/10.3390/biomass3020009

Neves, D., Thunman, H., Matos, A., Tarelho, L., & Gómez-Barea, A. (2011). Characterization and prediction of biomass pyrolysis products. *Progress in Energy and Combustion Science*, *37*(5), 611-630. https://doi.org/10.1016/j.pecs.2011.01.001

Nguyen, H. N. (2024). Integrated CO2-hydrothermal carbonization and high temperature steam gasification of bamboo feedstock: A comprehensive experimental study. *Advances in Bamboo Science*, *6*, 100060. https://doi.org/10.1016/j.bamboo.2024.100060

Nguyen, N. M., Alobaid, F., & Epple, B. (2021). Process simulation of steam gasification of torrefied woodchips in a bubbling fluidized bed reactor using Aspen plus. *Applied Sciences*, *11*(6), 2877. https://doi.org/10.3390/app11062877

Pala, L. P., Wang, Q., Kolb, G., & Hessel, V. (2017). Steam gasification of biomass with subsequent syngas adjustment using shift reaction for syngas production: An Aspen plus model. *Renewable Energy*, *101*, 484-492. https://doi.org/10.1016/j.renene.2016.08.069

Puig-Gamero, M., Pio, D., Tarelho, L., Sánchez, P., & Sanchez-Silva, L. (2021). Simulation of biomass gasification in bubbling fluidized bed reactor using Aspen plus®. *Energy Conversion and Management*, *235*, 113981. https://doi.org/10.1016/j.enconman.2021.113981

Salas, D., Boero, A., & Ramirez, A. (2024). Life cycle assessment of bioenergy with carbon capture and storage: A review. *Renewable and Sustainable Energy Reviews*, *199*, 114458. https://doi.org/10.1016/j.rser.2024.114458

Shahbeig, H., Shafizadeh, A., Rosen, M. A., & Sels, B. F. (2022). Exergy sustainability analysis of biomass gasification: A critical review. *Biofuel Research Journal*, *9*(1), 1592-1607. https://doi.org/10.18331/brj2022.9.1.5

Siwal, S., Zhang, Q., Sun, C., Thakur, S., Kumar Gupta, V., & Kumar Thakur, V. (2020). Energy production from steam gasification processes and parameters that contemplate in biomass gasifier – A review. *Bioresource Technology*, *297*, 122481. https://doi.org/10.1016/j.biortech.2019.122481

Wang, Z., Zhang, B., & Qi, G. (2020). Research status and analysis of biomass pyrolysis gasification technology. *IOP Conference Series: Materials Science and Engineering*, *721*(1), 012075. https://doi.org/10.1088/1757-899x/721/1/012075

Winchell, L. J., Ross, J. J., Brose, D. A., Pluth, T. B., Fonoll, X., Norton, J. W., & Bell, K. Y. (2022). Pyrolysis and gasification at water resource recovery facilities: Status of the industry. *Water Environment Research*, *94*(3). https://doi.org/10.1002/wer.10701

Xiang, Y., Cai, L., Guan, Y., Liu, W., Cheng, Z., & Liu, Z. (2020). Study on the effect of gasification agents on the integrated system of biomass gasification combined cycle and Oxy-fuel combustion. *Energy*, *206*, 118131. https://doi.org/10.1016/j.energy.2020.118131

Zaman, S. A., & Ghosh, S. (2021). A generic input–output approach in developing and optimizing an Aspen plus steam-gasification model for biomass. *Bioresource Technology*, *337*, 125412. https://doi.org/10.1016/j.biortech.2021.125412

Zhang, Y., Ji, Y., & Qian, H. (2021). Progress in thermodynamic simulation and system optimization of pyrolysis and gasification of biomass. *Green Chemical Engineering*, *2*(3), 266-283. https://doi.org/10.1016/j.gce.2021.06.003

Zhang, Y., Wan, L., Guan, J., Xiong, Q., Zhang, S., & Jin, X. (2020). A review on biomass gasification: Effect of main parameters on char generation and reaction. *Energy & Fuels*, *34*(11), 13438-13455. https://doi.org/10.1021/acs.energyfuels.0c02900

تعزيز إنتاج الهيدروجين في تغويز نشارة خشب الصنوبر باستخدام الطرق العددية والتجريبية

أحمد جادو[1] ، تتيانا موروزوق[2] و جينمينج بان[3]

[1] قسم الهندسة الزراعية والنظم الحيوية – كلية الزراعة – جامعة المنصورة – مصر
[2] معهد هندسة الطاقة ـ جامعة برلين للتقنية ـ برلين ـ ألمانيا
[3] قسم هندسة النظم الحيوية – جامعة تشجيانغ – هانغتشو – الصين

الملخص

يقدم هذا البحث دراسة شاملة لتحسين إنتاج الهيدروجين في عملية تغويز نشارة خشب الصنوبر من خلال المحاكاة العددية المتكاملة والتحقق التجريبي. أظهر النموذج العددي، الذي تم تطويره باستخدام برنامج ASPEN PLUS ، ترابطاً استثنائياً مع البيانات التجريبية (معامل التحديد 0.95 < R^2) عند درجة حرارة 800 درجة مئوية، مما يؤكد قدرته التنبؤية. كشف التحليل البارامتري أن رفع درجة حرارة التفاعل من 600 إلى 800 درجة مئوية أدى إلى تحسين كبير في تركيز الهيدروجين من 31.12 ٪ إلى 35.11 ٪ حجماً، ويرجع ذلك أساساً إلى تسارع تفاعلات تحول الغاز ـ الماء (WGS) وتفاعلات الإصلاح بالبخار الماصة للحرارة. أظهرت نسبة التكافؤ (ER) علاقة عكسية مع إنتاج الهيدروجين، حيث أدت زيادة نسبة التكافؤ من 0.2 إلى 0.4 إلى انخفاض كبير في تركيز الهيدروجين من 37.61 ٪ إلى 30.07 ٪ حجماً، ويُعزى ذلك إلى انخفاض توافر البخار لتفاعلات الإصلاح. علاوة على ذلك، أدى رفع نسبة البخار إلى الكتلة الحيوية (S/B) من 0.5 إلى 1.7 إلى زيادة في تركيز الهيدروجين من 35.28 ٪ إلى 37.22 ٪ حجماً، وذلك بسبب تحسين حركية تفاعلات الإصلاح بالبخار وتفاعلات تحول الغاز ـ الماء. من خلال التحسين متعدد المعايير، تم تحديد الظروف المثلى عند درجة حرارة: 750- 800 درجة مئوية، ونسبة تكافؤ 0.25-0.2 : ، ونسبة البخار إلى الكتلة الحيوية : 1.1- 1.4 ، ، مما حقق تركيزات قصوى للهيدروجين تتراوح بين 38-36 ٪ حجماً.